

# Photophysical comparative study of amylose and polyvinylpyrrolidone / single walled carbon nanotubes complex.

P. Bonnet <sup>a,b\*</sup>, J.P. Buisson <sup>a</sup>, N. Nomède Martyr <sup>a</sup>, H. Bizot <sup>c</sup>, A. Buelon <sup>c</sup> and O. Chauvet <sup>a</sup>

a - Institut des Matériaux Jean Rouxel, UMR6502, Université de Nantes - CNRS, 2 rue de la Houssinière, 44322 Nantes cedex 3, France

b - Laboratoire des Matériaux Inorganiques, UMR6002, Université Blaise Pascal Clermont-Ferrand 2 - CNRS, 24 Avenue des Landais, 63177 Aubière cedex, France

c - INRA-BIA, site de Nantes, Rue de la Géraudière BP 71627 - 44316 Nantes cedex 3, France

\* Corresponding Author : [pierre.m.bonnet@univ-bpclermont.fr](mailto:pierre.m.bonnet@univ-bpclermont.fr)

## ABSTRACT:

Progressive addition of hydroxypropylated amylose (AmH), from 0.05 wt% to 4.5 wt%, to single-walled carbon nanotubes (SWNTs) in aqueous surfactant suspensions quenches the intrinsic near-Infra-Red fluorescence of semiconducting SWNTs while dispersions obtained with a same amount of polyvinylpyrrolidone (PVP) remain luminescent. Near Infra-Red emission spectroscopy (fluorescence and Raman scattering) of the samples is used to characterize the supramolecular organization of these polymer/SWNT complex. The SWNTs are found to be wrapped by the PVP chains and not by the AmH chains which rather form AmH/surfactant/SWNTs complex. In PVP/SWNTs dispersion, the fluorescence line position and intensity are affected by dielectric screening. In the case of AmH/surfactant/SWNTs complex, dielectric screening plays also a role but quenching occurs above about 3 wt % of AmH. We attribute the quenching to the formation of a “composite like” microstructure by opposition to stabilized dispersion.

## INTRODUCTION:

The first report of near Infra-Red (NIR) fluorescence of Single Walled Carbon Nanotubes (SWNTs) by O'Connell et al. in 2002<sup>1</sup> has initiated a worldwide large research effort. Basic studies attempt to characterize and to understand the fundamental phenomena that drive the optical properties (electronic structure, excitonic decay and splitting...). Some other works are also using these peculiar optical properties for device applications (optoelectronic, sensors, etc.)<sup>2,3,4</sup>. As already shown by O'Connell et al, NIR fluorescence is only observed when the SWNTs are isolated: the interactions of the SWNTs with their environment but also an intrinsically low quantum yield ( $Q < 10^{-3}$ ) are critical for emission<sup>1,5,6</sup>. Indeed a controlled increase of the quantum yield may be very

important for optoelectronic applications of the SWNTs. The elaboration of luminescent polymer/SWNT complexes or composites can be a way to modify the quantum yield, and multifunctional applications can be envisioned for these materials in the future. In order to prepare these composites, covalent or non-covalent functionalization of SWNTs by polymers may be used. Functionalization of SWNTs is used for SWNTs dispersion, isolation and selectivity<sup>7,8,9</sup>, for production of SWNTs-based composites and for tailoring their properties<sup>10,11</sup>, for elaboration of sensors or devices for energy and optoelectronic applications<sup>12,13,14</sup> or for biological applications<sup>13,15,16</sup>. Non covalent functionalization is especially interesting since it preserves the structural integrity of SWNTs and thus their physical properties, and also because it is reversible.

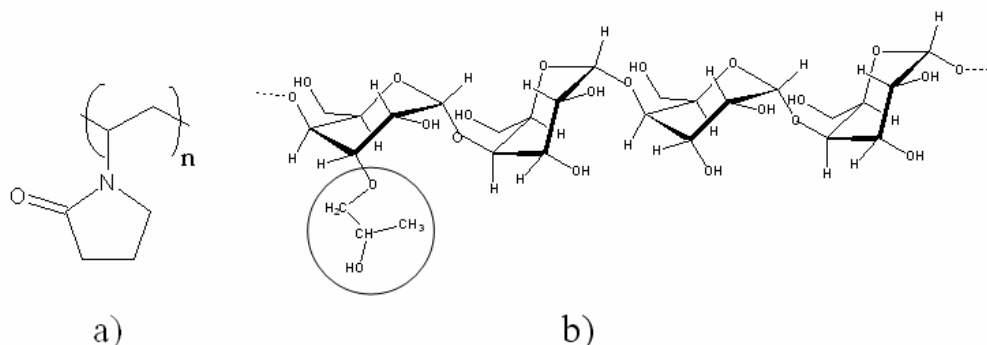


**FIGURE 1:** Chemical structures of (a): PVP; (b): Hydroxypropylated amylose (AmH). The circle shows the hydroxypropyl side group.

**Table 1:** Compositions of the AmH/SWNT and PVP/SWNT complex.

<i>Polymers</i>	<i>Contents (wt %)</i>							
<i>AmH</i>	0.05	0.1	0.2	0.5	1.0	2.3	3.3	4.5
<i>PVP</i>	0.05	--	0.2	--	--	2	3	4.5

The purpose of this paper is to show that the optical properties of polymer/SWNT complex are influenced by the complex supramolecular structure and by the interaction between the polymer chains and the SWNTs. Here we compare amylose derivative/SWNT and PVP/SWNT complexes where amylose is a polysaccharide biopolymer and PVP is (synthetic) polyvinyl pyrrolidone. These two different polymers have been chosen because they were supposed to wrap the SWNTs. Actually, these polymer/SWNT complexes exhibit quite different optical properties and we show that these is because they have different microstructures. Indeed, it shows that the supramolecular organization of the polymer/SWNT complex is a key point for potential applications based on the SWNTs optical properties.

## EXPERIMENTAL SECTION:

As-produced HiPCO SWNTs (from Carbon Nanotech. Inc.) have been dispersed in D<sub>2</sub>O

(mg.cm<sup>-3</sup>) in presence of Sodium Dodecyl Benzensulfonate (SDBS) (0.7wt%) following the procedure of ref. 17. After sonication and ultracentrifugation (120000g for 2h), isolated SWNTs suspended in SDBS micelles are obtained in the suspension. Hydroxypropylated Amylose (AmH) (Amylose from Aldrich, purified by butanol precipitation and hydroxypropylated at INRA Nantes<sup>18</sup>, M<sub>w</sub> =360000) or Polyvinyl Pyrrolidone (PVP) (from Aldrich, M<sub>w</sub> =360000) have been added to the suspensions. AmH and PVP chemical formula are given in Figure 1. Once the polymer is introduced in the suspension, the mixture is sonicated for 10 h in a water bath. The polymer content, [AmH] or [PVP] respectively, varies between 0 to 4.5 wt% as shown in Table 1. When needed, PVP/SWNT and AmH/SWNT suspensions have been dialyzed with a spectrapor MWCO 12-14000 membrane (from Spectrumlabs) against water and an ion retardation resin (AG11A8 from BioRad) for 48h in order to remove the SDBS surfactant.

Photoluminescence (PL) and Raman scattering spectra of the suspensions have been obtained with a RFS 100 Bruker FT Raman spectrometer using an excitation line at 1064 nm (1.16 eV). The detector of the spectrometer allows to detect emitted or scattered photons with energy between 0.85 and 1.16 eV.

## RESULTS AND DISCUSSIONS:

### 1 – Structure:

Homogeneous and black suspensions are obtained for the PVP/SWNT mixtures whatever the amount of PVP. Homogeneous suspensions are also obtained with AmH as long as  $[AmH] < 1$  wt % but a partial sedimentation is observed when  $[AmH] > 1$  wt %<sup>19</sup>. Indeed, the stability of the suspensions suggests that the SWNT are isolated and protected from the aqueous environment in the solution. It has already been shown<sup>1,7,20,21</sup> that PVP can wrap individual SWNTs with several possible microstructures including double and triple helix<sup>7</sup>. Amylose is also considered as a wrapping agent of SWNTs<sup>22,23</sup>.

One way to probe the interaction of the SWNTs with their environment is to investigate their optical properties. Figure 2 shows the near infra-red fluorescence spectrum of the SWNTs dispersed in SDBS before the introduction of the polymers in the solution, in the energy range 0.85-1.16 eV and with an excitation at 1.16 eV. NIR fluorescence of nanotubes is due to the radiative recombination of the  $S_{11}$  singlet excitonic states<sup>24,25</sup>. The fluorescence peaks can be assigned to (9,4) (12,1) (11,3) (10,3) and (8,7) SWNTs following Bachilo et al<sup>26</sup>. The stars on the spectrum indicate the Raman G bands and RBM bands of the nanotubes. These SWNTs have diameters between 0.89 and 1.02 nm. The strong fluorescence observed in Figure 2 shows that the SWNTs are individualized by the strong ultrasonic and ultracentrifugation treatment in presence of SDBS before the introduction of the polymers.

Figure 3 shows the emission spectra of AmH/SWNT (left panel) and PVP/SWNT (right panel) suspensions (for 0.05, 2 and 4.5 wt %) before (curve 1) and after dialysis (curve 2). Before dialysis and for a polymer amount of 0.05 wt%, the spectra reveal both fluorescence bands (broad bands) and Raman bands (sharp bands, labelled with stars). The spectrum of AmH/SWNT is very close to the

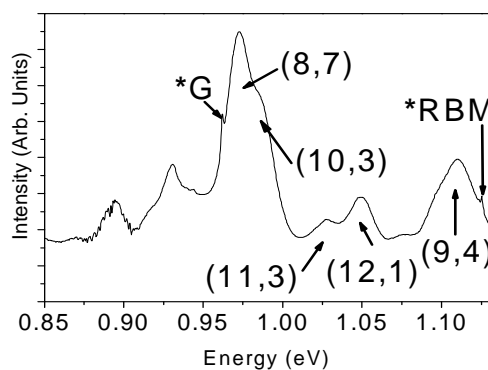


**FIGURE 2:** Emission spectrum obtained from an ensemble of suspended SWNTs in SDBS micelles with a laser excitation at 1064 nm (1.16 eV). The stars label the Raman RBM and G peaks.

spectrum of free suspended SWNTs in SDBS micelles (cf Figure 2). When the amount of amylose increases, the PL bands loose their intensity and for  $[AmH]=4.5$  wt%, fluorescence from (9,4) and (8,7) tubes becomes difficult to observe. Upon dialysis, the PL bands disappear for all  $[AmH]$  content and only the Raman bands remain visible. The situation is different for PVP/SWNT. For  $[PVP]=0.05$  wt%, both fluorescence and Raman bands are visible but the fluorescence bands are shifted by comparison with Figure 2. In this case, dialysis leads to a frequency shift of the PL bands and quite a small reduction of their intensity. When the amount of PVP increases, there is no significant evolution of the emission spectra before or after dialysis. The intensity of the fluorescence bands does not seem to depend on  $[PVP]$  and dialysis results in quite a strong redshift of the PL bands.

The behaviour observed for PVP/SWNT is a signature of the wrapping ability of PVP. The addition of PVP to the SWNTs suspension in SDBS micelles induces a redshift of the PL peaks and a small loss of intensity. This shift is independent of the amount of PVP. It is due to the modification of the exciton energy with the wrapping of PVP directly around the SWNTs which causes a change of effective dielectric constant<sup>27,28</sup>. The microstructure of PVP wrapped SWNTs does not change with

further additions of PVP unlike in the case of AmH addition. When SDBS is removed, a further  $16 \pm 4\text{meV}$  redshift and a loss of intensity are observed. It means that SDBS was still in contact with the nanotubes. When adding PVP into the SDBS stabilized SWNTs dispersion, it is likely that PVP has not been exchanged completely with SDBS. A part of the SWNTs surface is not covered by the polymer but by the surfactant. The dialysis removes the remaining SDBS, leaving SWNTs wrapped by PVP in the solution.

The situation is different in presence of AmH. There is an absence of shift for  $[\text{AmH}] = 0.05\%$  which shows that AmH is not in close contact with the SWNTs surface and conversely that SDBS is still covering a large part of the surface. With further addition of AmH, fluorescence is progressively quenched and it shifts progressively towards the red. The quenching of fluorescence is likely related to a (partial) sedimentation of the AmH/SWNT dispersion

when more than 1 wt% of AmH is added into the SWNT suspension<sup>19</sup>. Please note also that a sedimentation of the suspensions is also observed when dialysis sets in AmH/SWNT dispersion. It means that AmH is not able to wrap the nanotubes, presumably because it interacts with the surfactant and three centers AmH/SWNTs/SDBS complexes are formed<sup>17,19</sup>. PVP/SWNT and AmH/SWNT complexes may thus have different microstructure as reflected by the sedimentation and the fluorescence behaviour.

The supramolecular organization of the PVP/SWNT and AmH/SWNT complex are thus very different. In the first hand, PVP wraps individual SWNTs as described in the literature<sup>7,20</sup> and PVP wrapped SWNTs complex are soluble. In the second hand individual SWNTs are coated by AmH but SDBS is still necessary to stabilize water soluble complex. We suggest that SDBS interacts with the AmH/SWNT complex

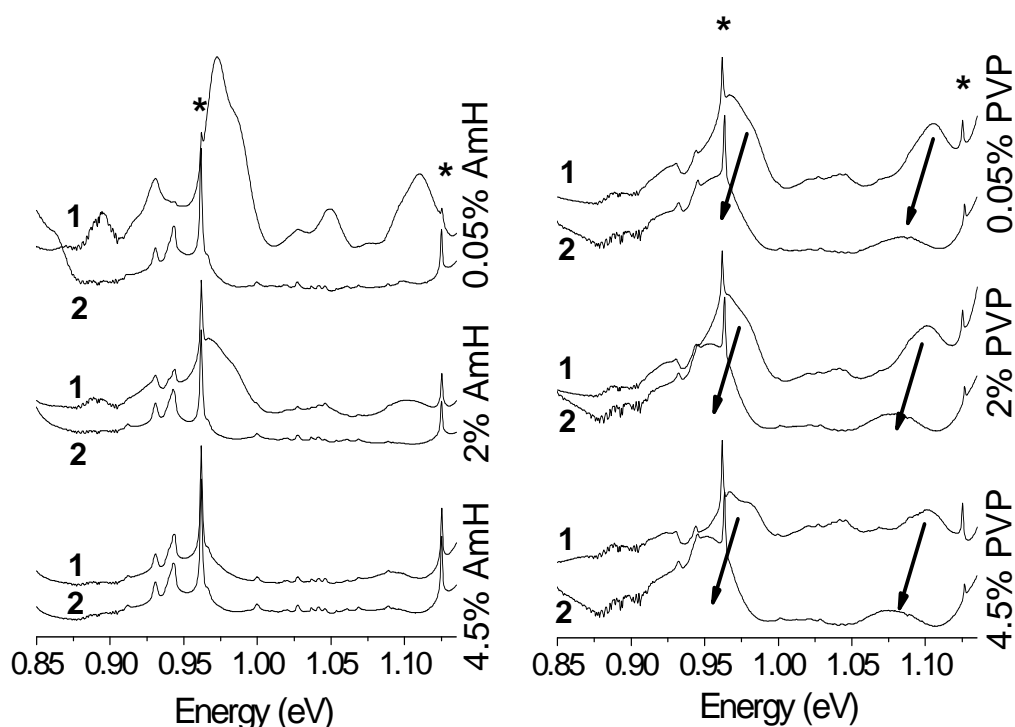


**FIGURE 3:** (Left panel) Emission spectra of AmH/SWNT complex with  $[\text{AmH}] = 0.05, 2.3$  and  $4.5$  wt % from top to bottom respectively. (Right panel) Emission spectra of PVP/SWNT complex with  $[\text{PVP}] = 0.05, 2.0$  and  $4.5$  wt % from top to bottom respectively. Spectra labelled “1” correspond to the as produced complex. Spectra labelled “2” are obtained after the dialysis of the dispersion. They are free of SDBS. The stars indicate the Raman G band and the RBM band, the arrows underline the PL peak shifts induced by the dialysis treatment.

through its alkyl part which fills the hydrophobic gap of the AmH helix<sup>29</sup>. This interaction leads to the formation of a three centers SDBS/AmH/SWNT complex<sup>17,19</sup>. The putative structures of PVP/SWNT and the SDBS/AmH/SWNT complex are sketched in Figure 4. Monte Carlo simulations<sup>30</sup> have shown that the flexible polymers chains, like PVP<sup>31</sup>, can wrap around individual SWNTs, while the helical conformation of AmH is not flexible enough to allow wrapping. SDBS/AmH inclusion complex are thus more easily formed. In situ polymerization of amylose around SWNTs, as proposed by Yang et al., may be a more efficient route for a direct wrapping<sup>32</sup>.

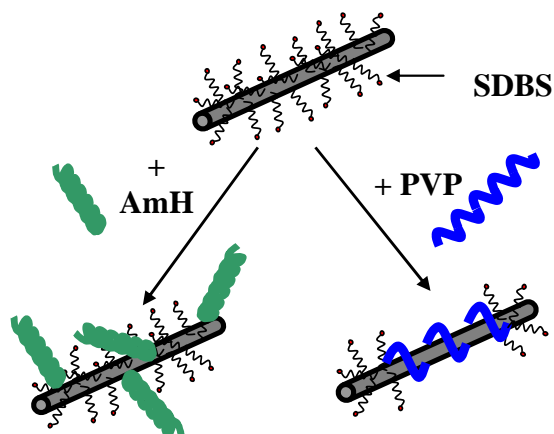


**FIGURE 4:** Sketch of the microstructure of AmH/SWNT and PVP/SWNT complex in presence of SDBS at low contents of polymer ( $\leq 1$  wt%). AmH chains make inclusion complex with the SDBS alkyl part at the surface of the SWNTs. PVP chains wrap the SWNT.

## 2 - Optical properties of the dispersions:

As shown in Figure 3, the optical characteristics of the SWNTs are very sensitive to their environment. In order to be more quantitative, the emission spectra have been fitted with lorentzian lines associated to the fluorescence peaks. An example is shown in Figure 5. It allows to extract the positions, the linewidths and the intensities of the fluorescence peaks. In Figure 6, the position of the (9,4) and (8,7) fluorescence peaks and the intensity of the (9,4), (12,1), (11,3), (10,3) and (8;7) peaks are plotted versus the

polymer content. The peak intensities are normalized to the Raman G peaks and for each chirality (n,m) the maximal intensity is normalized to 1. According to Moore et al.<sup>33</sup>, the SWNT fluorescence peak to Raman G-peak intensity ratio gives a qualitative measure of the energy transfer of the excited state to the surroundings.

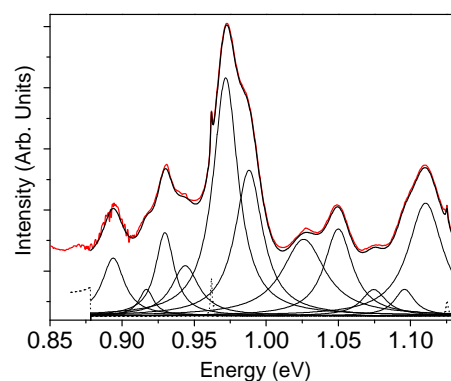


**FIGURE 5:** Experimental (red line) and fitted (black line) spectra of AmH/SWNT complex at [AmH]=0.1wt%. Individual SWNTs fluorescence peaks are fitted with Lorentzian profiles.

In Figure 5, the PL peak position shifts about 20 meV for [AmH] = 4.5wt% and about 9 meV for [PVP] = 4.5 wt % for (9,4) SWNTs. These values are consistent with the shifts reported for PVP<sup>7,20</sup>, DNA<sup>34</sup> or gelatine<sup>35</sup>. This red shift is a direct consequence of the dielectric screening of the coulomb interaction in SWNT by its environment. The exciton energy is the sum of two main terms: the direct Coulomb interaction which drives the binding energy of the exciton ( $E_B \propto \epsilon^{-\alpha}$  where  $\epsilon$  is the effective dielectric constant and  $\alpha \sim 1.4$ <sup>27</sup>) and the exchange interaction which drives the exchange energy ( $E_{ex} \propto \epsilon^{-\beta}$  with  $\beta=1$ <sup>28</sup>). These two terms have opposite contributions on the value of the exciton energy, a positive one for the exchange interaction and a negative one for the Coulomb interaction<sup>28</sup>. When the effective dielectric constant is modified, the exciton energy changes as

$$\Delta E = (\Delta \epsilon / \epsilon) \times (\alpha E_B - \beta E_{ex}). \quad (1)$$

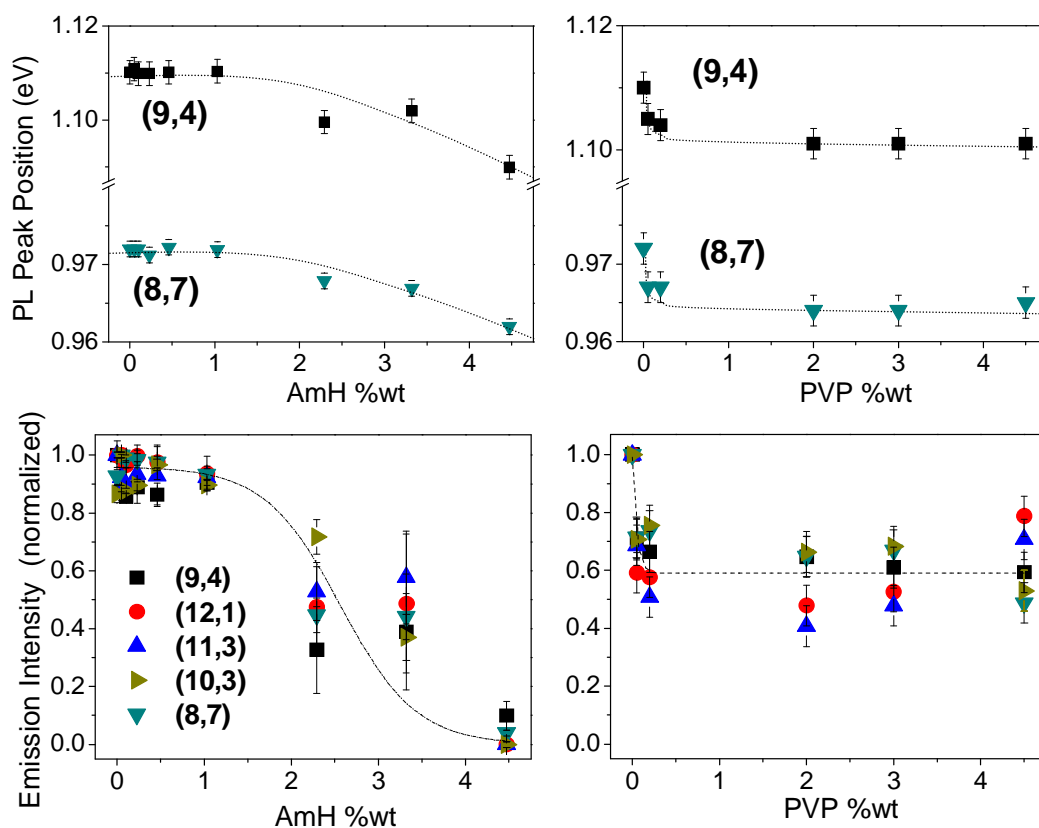


**FIGURE 6:** (Upper panel): Shift of the PL peak positions of the (9,4) and (8,7) SWNT versus the polymer content for AmH (left) and PVP (right). (Lower panel): Normalized PL intensity evolution versus the polymer content for AmH (left) and PVP (right). The dashed lines are guides for the eyes.

In SWNTs the exchange interaction is stronger than the Coulomb interaction, and thus an increase of the dielectric constant leads globally to a red shift of the PL peaks<sup>28</sup>.

Dukovic et al.<sup>36</sup> have estimated the binding energy of the SWNT exciton from two-photon photoluminescence excitation spectroscopy (PLE). For a (9,4) SWNT with a diameter of 0.92 nm,  $E_B$  is found to be of the order of 370 meV. Lefebvre et al.<sup>28</sup> have estimated the exchange energy of a nanotube with the same diameter and they have found about 660 meV. Using these values in formula (1) and the shifts extracted from Figure 5 leads to a relative change of the dielectric constant of about  $\Delta\epsilon/\epsilon \sim 14\%$  and 6% for 4.5% of AmH and PVP respectively. The red shifts for the (8,7) SWNTs are smaller because  $E_B$  and  $E_{ex}$  decrease when the SWNT diameter increases<sup>28,36,37</sup>.

It is worth noting the important differences in the dependence of the PL peaks positions with the amount of AmH and PVP. This is the signature of the different microstructure of the PVP/SWNTs or AmH/SWNTs complex. Addition of only 0.05 wt% of PVP results in a strong shift of about 8 meV while further addition does not shift any more the lines. The rapid shift of the line suggests that a small quantity of PVP is sufficient to wrap the individual SWNTs.

Conversely, adding less than 1% of AmH does not shift the fluorescence lines. Below 1wt% the interaction between AmH and SWNTs seems thus to be weak. It is attributed to a supra molecular structure where the SWNT is still in contact with the SDBS surfactant, the AmH helix being essentially in contact with the surfactant alkyl queue. As a consequence the direct environment, and thus the effective dielectric

constant, of the SWNTs is not modified. The shift of the PL line starts to happen above  $[AmH]=1\%$ . It corresponds to the quantity above which sedimentation occurs. We argue that this concentration plays an equivalent role to a critical micellar concentration: isolated AmH chains complexified by SWNTs/SBDS are no more stable in water and AmH chains tend to aggregate. The SWNTs/SBDS complex are glued in a AmH polymer network similar to a composite. The transition from free AmH/SBDS/SWNT complex to embedded SWNTs causes an important change of dielectric constant ( $\sim 14\%$ ).

The evolution of the fluorescence line position is also reflected in the evolution of the normalized fluorescence intensities of PVP/SWNT and AmH/SWNT suspensions (see lower panel of Figure 6). The introduction of 0.05wt% of PVP reduce by  $\sim 40\%$  the PL intensity relative to free micelles suspended SWNTs, after which no important modifications are noticed for higher concentrations in PVP. When SWNTs are wrapped by PVP, the change of dielectric constant changes also the exciton energy. It results in a modification in the resonance conditions which leads to a decrease in the PL intensities. It can be noticed that within our experimental accuracy, this process does not seem to be selective in chiralities since the five fluorescence lines behave quite in the same way.

It is very different with AmH where the fluorescence intensity remains constant below 1% of AmH and it decreases strongly at 2%. Fluorescence is fully quenched at 4.5%. Quenching of fluorescence cannot be only attributed to the modification of the resonance conditions as discussed above. First, addition of PVP changes also the resonance conditions and the fluorescence survives. Furthermore, important line shifts have also been reported in the literature without quenching: Chou et al. report a  $\sim 28$  meV red shift relative to SDS stabilized SWNTs for (9,4) SWNTs engaged in DNA/SWNT and the fluorescence is still

effective<sup>34</sup>. In our case and as shown in Figure 3 after dialysis, the (9,4) SWNTs PL peak is red shifted by 33 meV with  $[PVP]=4.5\text{wt}\%$  of PVP by comparison with SDBS/SWNT dispersion.

**Table 2:** Possible Donors-Acceptors couples in an exciton energy transfer process.

<i>Donors</i>	<i>Acceptors</i>
(10,2)	(9,4); (12,1); (11,3); (10,3); (8,7)
(9,4)	(12,1); (11,3); (10,3); (8,7)
(12,1)	(11,3); (10,3); (8,7)
(11,3)	(10,3); (8,7)
(10,3)	(8,7)

Two other mechanisms can be invoked to explain the loss of fluorescence. A self quenching process may occur by exciton energy transfer (EET) between close enough nanotubes. The exciton desexcitation may also be mediated in a non radiative way via the AmH chains. The EET process consists of the transfer of the exciton energy from an excited SWNT (donor) to a neighbouring SWNT (acceptor). It requires that the two SWNTs are close enough together and that there is a spectral overlap between the donor emission and the acceptor absorption bands. Usually the EET is associated with an increase of the emission intensity of the acceptor. Förster resonance energy transfer (FRET) is the mechanism which is the most commonly invoked for SWNTs<sup>38,39,40</sup>. The FRET efficiency is proportional to  $R_{DA}^{-6}$  where  $R_{DA}$  is the intertube distance. Indeed the formation of the AmH/SWNT “composite” structure increases the local concentration of SWNTs and thus it may enhance the probability of EET. In table 2, we have listed some possible donor-acceptor couples concerned by this process for semiconducting couples: the SWNT donor bandgap must be larger than the SWNT acceptor one. It should also be added that EET to a metallic tube is likely which results in a absence of fluorescence. As can be seen in Figure 3 and Figure 5, there is a general decrease of the fluorescence and it does not

seem that there is a transfer from one kind of semiconducting tubes to another. It suggests that the FRET mechanism is not responsible for the quenching of the fluorescence and the quenching is mainly due to a non radiative desexcitation of the exciton through the polymer chains. Such a process is likely related to the broadening of the PL lines that is observed when [AmH] increases. For instance the (8,7) PL line broadens by about 8.5 meV when 3.3% of AmH is introduced (it corresponds to a relative broadening of 46%). The broadening is the signature of the coupling to the vibrational modes of AmH. In summary, we argue that below 2%, the optical properties of the AmH/SWNT dispersion are mainly driven by the dielectric screening, while above 3% quenching of the fluorescence is mainly caused by a strong coupling with the vibrational modes of the AmH network.

## CONCLUSION:

In Summary, PVP/SWNT and AmH/SWNT complex have been prepared in aqueous solutions in presence of SDBS surfactant. The NIR fluorescence of the PVP/SWNT complex is quite independent of the amount of PVP, unlike the case of the AmH/SWNT complex. We attribute these different behaviours to the two distinct microstructures of the complexes. With PVP, a wrapping of the SWNTs occurs while with AmH, the situation is more intricate: at low content, isolated three-body complexes are formed while at high content a composite structure is obtained. The influence of polymers molecular weight and the functionalisation degree of amylose on the polymer/SWNT complex microstructures is under investigation.

The emission properties of the PVP/SWNT complex are driven by the dielectric screening resulting from the addition of PVP to the SWNT suspensions. This is also the same for AmH/SWNT complex below [AmH] = 2%. Above this quantity of AmH, the quenching of the fluorescence is

observed. We argue this is due to the coupling of the excitonic states with the vibrational modes of the polymer network and the AmH/SWNT composite microstructure.

This paper shows that the optical properties are efficient probes of the microstructures of polymers/SWNT complexes. It can be helpful for optoelectronic or sensing applications.

\*\*\*\*\*

## REFERENCES:

1. M.J. O'Connell, S.M. Bachilo, C.B. Huffman, V.C. Moore, M.S. Strano, E.H. Haroz, K.L. Rialon, P.J. Boul, W.H. Noon, C. Kittrell, J. Ma, R.H. Hauge, R.B. Weisman, and R.E. Smalley, *Science*, 2002, **297**, 593.
2. E. Adam, C. M. Aguirre, L. Marty, B.C. St-Antoine, F. Meunier, P. Desjardins, D. Menard and R. Martel, *Nano Lett.*, 2008, **8**, 2351
3. Ph. Avouris, J. Chen, M. Freitag, V. Perebeinos, and J. C. Tsang, *Phys. Status Solidi b*, 2006, **243**, 3197
4. P.W. Barone, S. Baik, D.A. Heller and M.S. Strano, *Nat. Mater.*, 2004, **4**, 86
5. F. Wang, G. Dukovic, L. E. Brus, and T. F. Heinz, *Phys. Rev. Lett.*, 2004, **92**, 177401
6. J.S. Lauret, C. Voisin, S. Berger, G. Cassabois, C. Delalande, Ph. Roussignol, L. Goux-Capes and A. Filoramo, *Phys. Rev. B*, 2005, **72**, 113413
7. M.J. O'Connell, P. Boul, L.M. Ericson, C. Huffman, Y. Wang, E. Haroz, C. Kuper, J. Tour, K. D. Ausman and R. E. Smalley, *Chem. Phys. Lett.*, 2001, **342**, 265
8. Y-T. Liu, W. Zhao, Z-Y. Huang, Y-F. Gao, X-M Xie, X-H. Wang and X-Y. Ye, *Carbon*, 2006, **44**, 1581
9. J-B. Kim, T. Premkumar, K. Lee and K.E. Geckeler, *Macromol. Rapid Commun.*, 2007, **28**, 276
10. C. Bartholome, P. Miaudet, A. Derré, M. Maugey, O. Roubeau, C. Zakri and P. Poulin, *Compos. Sci. Technol.*, 2008, **68**, 2568
11. J.Q. Liu, T. Xiao, K. Liao and P.Wu, *Nanotechnology*, 2007, **18**, 165701
12. A. Star, V. Joshi, T-R. Han., M. Virginia, P. Altoe, G. Grulner and J. F. Stoddart, *Org. Lett.*, 2004, **6**, 2089
13. S. R. Shin, C. K. Lee, I. So, J-H. Jeon, T. M. Kang, C. Kee, S. I. Kim, G. M. Spinks, G. G.

- Wallace and S. J. Kim, *Adv. Mater.*, 2008, **20**, 466
14. J.-H. Ryu, T. Nagamura, M. Shigeta and N. Nakashima, *Macromol. Symp.*, 2006, **242**, 193
  15. Y. Lin, S. Taylor, H. Li, K. A. S. Fernando, L. Qu, W. Wang, L. Gu, B. Zhou and Y.-P. Sun, *J. Mater. Chem.*, 2004, **14**, 527
  16. A. Bianco, K. Kostarelos, C. D. Partidos and M. Prato, *Chem. Commun.*, 2005, 571
  17. P. Bonnet, D. Albertini, H. Bizot, A. Bernard and O. Chauvet, *Compos. Sci. Technol.*, 2007, **67**, 817
  18. G. Wulff, A. Steinert, O. Höller, *Carbohydr. Res.*, 1998, **307(1-2)**, 19
  19. P. Bonnet, M. Grésil, H. Bizot, I. Riou, P. Bertoncini, C. Harb, A. Buleon and O. Chauvet, hal-00363697, 2009
  20. L.-J. Li, R. J. Nicholas, C.-Y. Chen, R.C. Darton and S.C. Baker, *Nanotechnology*, 2005, **16**, S202 ; L.J. Li, R.J. Nicholas, R.S. Deacon and P.A. Shield, *Phys. Rev. Lett.*, 2004, **93**, 156104
  21. V.V. Didenko, V.C. Moore, D.S. Baskin and R.E. Smalley, *Nano Lett.*, 2005, **5 (8)**, 1563
  22. A. Star, D.W. Steuerman, J.R. Heath and J.F. Stoddart, *Angew. Chem. Int. Ed.*, 2002, **41**, 2618
  23. O.-K. Kim, J. Je, J.W. Baldwin, S. Kooi, P.E. Pehrsson and L.J. Buckley, *J. Am. Chem. Soc.*, 2003, 125, 4426
  24. F. Wang, G. Dukovic, L.E. Brus and T.F. Heinz, *Science*, 2005, **308**, 838
  25. J. Maultzsch, R. Pomraenke, S. Reich, E. Chang, D. Prezzi, A. Ruini, E. Molinari, M. S. Strano, C. Thomsen, and C. Lienau, *Phys. Rev. B*, 2005, **72**, 241402 ( R )
  26. S.M. Bachilo, M.S. Strano, C. Kittrell, R.H. Hauge, R.E. Smalley and R.B. Weisman, *Science*, 2002, **298**, 2361
  27. V. Perebeinos, J. Tersoff, and P. Avouris, *Phys. Rev. Lett.*, 2004, **92**, 257402
  28. J. Lefebvre and P. Finnie, *Nano Lett.*, 2008, **8**, 1890
  29. M. Egermayer and L. Piculell, *J. Phys. Chem. B*, 2003, **107**, 14147
  30. I. Gurevitch and S. Srebnik, *Chem. Phys. Lett.*, 2007, **444**, 96
  31. A.M. Tedeschi, E. Busi, R. Basosi, L. Paduano and G. D'Errico, *J. Solution Chem.*, 2006, **35**, 951
  32. L. Yang, B. Zhang, Y. Liang, B. Yang, T. Kong and L.-M. Zhang, *Carbohydr. Res.*, 2008, **343**, 2463
  33. V.C. Moore, M.S. Strano, E.H. Haroz, R.H. Hauge, and R.E. Smalley, *Nano Lett.*, 2003, **3(10)**, 1379
  34. S.G. Chou, H.B. Ribeiro, E.B. Barros, A.P. Santos, D. Nezich, Ge.G. Samsonidze, C. Fantini, M.A. Pimenta, A. Jorio, F. Plentz Filho, M.S. Dresselhaus, G. Dresselhaus, R. Saito, M. Zheng, G.B. Onoa, E.D. Semke, A.K. Swan, M.S. Unlu and B.B. Goldberg, *Chem. Phys. Lett.*, 2004, **397**, 296
  35. H. Hirori, K. Matsuda, Y. Miyauchi, S. Maruyama and Y. Kanemitsu, *Phys. Rev. Lett.*, 2007, **97**, 257401
  36. G. Dukovic, F. Wang, D. Song, M.Y. Sfeir, T.F. Heinz and L.E. Brus, *Nano Lett.* 2005, **5**, 2314
  37. Y. Ohno, S. Iwasaki, Y. Murakami, S. Kishimoto, S. Maruyama and T. Mizutani, *Phys. Status Solidi b*, 2007, **244**, 4002
  38. P.H. Tan, A.G. Rozhin, T. Hasan, P. Hu, V. Scardaci, W.I. Milne and A.C. Ferrari, *Phys. Rev. Lett.*, 2007, **99**, 137402
  39. H. Qian, C. Georgi, N. Anderson, A. A. Green, M. C. Hersam, L. Novotny and A. Hartschuh, *Nano Lett.*, 2008, **8**, 1363
  40. R.A. Graff, P. Swanson, P.W. Barone, S. Baik, D.A. Heller and M.S. Strano, *Adv. Mater.*, 2005, **8**, 980